Neuro-Oncology 15(11):1457–1468, 2013.
doi:10.1093/neuonc/not115
Advance Access publication September 5, 2013

Toll-like receptor 2 mediates microglia/brain macrophage MT1-MMP expression and glioma expansion

Katyayni Vinnakota*, Feng Hu*, Min-Chi Ku, Petya B. Georgieva, Frank Szulzewsky, Andreas Pohlmann, Sonia Waiczies, Helmar Waiczies, Thoralf Niendorf, Seija Lehnardt, Uwe-Karsten Hanisch, Michael Synowitz, Darko Markovic, Susanne A. Wolf, Rainer Glass, and Helmut Kettenmann

Cellular Neurosciences (K.V., F.H., M-C.K., P.B.G., F.S., S.A.W., R.G., H.K.) and Berlin Ultrahigh Field Facility, Max Delbrück Center for Molecular Medicine, Berlin, Germany (A.P., S.W., H.W., T.N.); Department of Neurology and Center for Anatomy, Institute of Cell Biology and Neurobiology, Charité Universitätsmedizin, Berlin, Germany (S.L.); Department of Neuropathology, University of Göttingen, Göttingen, Germany (U-K.H.); Department of Neurosurgery, Charité Universitätsmedizin, Berlin, Germany (M.S.); Department of Neurosurgery, Helios Clinic, Berlin, Germany (D.M.)

Present affiliation: Neurosurgical Research, Clinic for Neurosurgery, Ludwig Maximilians University of Munich, Munich, Germany (R. G.)

Background. Glioblastomas are the most aggressive primary brain tumors in humans. Microglia/brain macrophage accumulation in and around the tumor correlates with malignancy and poor clinical prognosis of these tumors. We have previously shown that microglia promote glioma expansion through upregulation of membrane type 1 matrix metalloprotease (MT1-MMP). This upregulation depends on signaling via the Toll-like receptor (TLR) adaptor molecule myeloid differentiation primary response gene 88 (MyD88).

Methods. Using in vitro, ex vivo, and in vivo techniques, we identified TLR2 as the main TLR controlling microglial MT1-MMP expression and promoting microglia-assisted glioma expansion.

Results. The implantation of mouse GL261 glioma cells into TLR2 knockout mice resulted in significantly smaller tumors, reduced MT1-MMP expression, and enhanced survival rates compared with wild-type control mice. Tumor expansion studied in organotypic brain slices depended on both parenchymal TLR2 expression and the presence of microglia. Glioma-derived soluble factors and synthetic TLR2 specific ligands induced MT1-MMP expression in microglia from wild-type mice, but no such change in MT1-MMP gene expression was observed in microglia from TLR2 knockout mice. We also found evidence that TLR1 and TLR6 cofunction with TLR2 as heterodimers in regulating MT1-MMP expression in vitro.

Conclusions. Our results thus show that activation of TLR2 along with TLRs 1 and/or 6 converts microglia into a glioma supportive phenotype.

Keywords: glioma, glioma-associated microglia/brain macrophages, MT1-MMP, TLR.

Gliomas are tumors of the CNS accounting for nearly 50% of all brain neoplasms, with an incidence of 7.3 per 100 000 persons per year.[1] Gliomas are caused by somatic mutations in neural stem and precursor cells, and glioma expansion can be promoted by the brain microenvironment, which supports pathological properties like angiogenesis, proliferation, migration, invasion, and survival.[2–4]

Microglia, the brain-resident macrophages, generally exhibit a ramified morphology in the healthy brain. Pathological insult leads to their activation and acquisition of ameboid morphology.[5] Despite similarity in morphology of activated microglial cells, their individual functions can be quite distinct.[6] Along with blood-borne macrophages, microglia contribute as much as 30% to the total tumor mass and are positively associated with

Received January 8, 2013; accepted June 23, 2013.

*These authors contributed equally to this work.

Corresponding Author: Prof Dr Helmut Kettenmann, PhD, Cellular Neurosciences, Max Delbrück Center for Molecular Medicine, Robert-Rössle-Str. 10, 13125 Berlin, Germany (kettenmann@mdc-berlin.de).

histopathological grade, malignancy, and invasiveness of gliomas.[7,8] Despite their cytotoxic and phagocytic function,[6,9] the immune function of glioma-associated microglia/brain macrophages (GAMs) is suppressed, thereby reflecting an M2-macrophage phenotype.[3,10] GAMs promote rather than suppress glioma expansion. Depletion of microglia reduced glioma invasion in organotypic brain slices[11] and decreased glioma expansion in vivo.[12] One important tumor-supportive mechanism is the upregulation of membrane type 1 matrix metalloprotease (MT1-MMP) in GAMs by glioma-derived soluble factor(s) that activate the Toll-like receptor (TLR) adaptor molecule myeloid differentiation primary response gene 88 (MyD88) and p38 mitogen-activated protein kinase (MAPK) in microglia.[12] Blocking this pathway has potential therapeutic benefits in glioma patients.[12,13]

TLRs belong to the superfamily of pattern recognition receptors that classically activate and mediate pro-inflammatory responses in innate immune cells by recognizing invading pathogens. They are type I transmembrane proteins, characterized by an extracellular domain of leucine-rich repeats and an intracellular Toll/interleukin (IL)-1 receptor domain. A total of 13 mammalian TLR orthologs (10 in humans and 12 in mice) have been described so far.[14,15] TLRs 1, 2, 4, 5, and 6 localize to the plasma membrane, while TLRs 3, 7, 8, and 9 are found in intracellular compartments of endosomes and lysosomes.[16] The expression and function of these receptors is also found not just in immune cells but also in nonimmune cells.[17] TLRs recognize conserved molecular signatures on microorganisms called pathogen-associated molecular patterns and rapidly alert the host to potential dangers.[15] Apart from their role in host defense mechanisms, TLRs 1, 2, 3, 4, 6, 7, and 9 have critical functions in pathologies like diabetes,[18,19] cancer,[20,21] cardiovascular diseases,[22,23] kidney diseases,[24,25] gastrointestinal diseases,[26,27] endocrine dysfuntionalities,[28] and CNS diseases.[29,30] In the present study, we identified TLR2 as one of the crucial TLRs that mediates the protumorigenic effect of microglia on glioma growth and expansion.

Materials and Methods

Animals

All in vitro, ex vivo, and in vivo experiments were done using C57Bl/6 wild-type (WT) mice (Charles River Laboratories) and TLR1, 2, 6, 7, and 9 knockout (KO) mice on a C57Bl/6 background. The TLR KO mice were generated by Dr Shizuo Akira and colleagues from Osaka University, Japan, and obtained from Oriental BioServices.[31–35] The mice were bred and maintained in the animal house facilities of the Max Delbrück Center and Charité University Hospital (Berlin, Germany) as per rules of the local governmental institutions. The mice were housed with a 12-h/12-h light/dark cycle and received food and water ad libitum. For all in vivo tumor inoculations, mice were anesthetized by i.p. injections of a 1.5% ketamine hydrochloride (Ketanest) and 0.1% xylazyne (Rompun) mixture in 0.9% NaCl. For perfusions followed by immunohistochemistry, tumor-bearing mice were anesthetized by i.p. injections of Narcoren. For estimation of tumor volume in vivo by MRI, mice were anesthetized with 2.8% isoflurane in an oxygen/air mixture (2:1) with a flow rate of 750 mL/min and maintained at 1.5%–2% for the entire experiment.

Cell Culture

Murine GL261 glioma cells (National Cancer Institute) were grown in Dulbecco's modified Eagle's medium (DMEM) with 10% fetal calf serum (FCS), 200 mM glutamine, 100 U/mL penicillin, and 100 μg/mL streptomycin (Invitrogen). Microglial cells were prepared from neonatal WT and TLR1, 2, 6, 7, and 9 KO mice according to previously established protocols.[11,36] Microglial cell cultures were used for experiments 1–2 days after plating. All cells were maintained in a 37°C incubator with a 5% CO_2 humidified atmosphere.

Microglia/Macrophage Isolation From Naïve and Tumor-bearing Mice

GAMs were acutely isolated from naïve and tumor-bearing WT and TLR2 KO mice 2 weeks after tumor inoculation for RNA isolation using magnetic beads as per the manufacturer's instructions (Miltenyi Biotec). Briefly, after anesthetization and decapitation of the mice, brains were removed, weighed, and enzymatically digested into single-cell suspension using the Neural Tissue Dissociation Kit (Miltenyi Biotec). The tissue was further dissociated, and debris was removed by applying a 40-μm cell strainer (Miltenyi Biotec). After removal of myelin with antimyelin beads, cell suspensions were incubated with CD11b microbeads in magnetic affinity cell sorting (MACS) buffer (PBS supplemented with 0.5% bovine serum albumin and 2 mM EDTA) for 10 min. The cells were then loaded onto a MACS column (Miltenyi Biotec), after washing of the column with MACS buffer. The CD11b-positive cells were eluted from the column. Then a fraction of the isolated cells were stained with CD11b antibody for fluorescence activated cell sorting analysis to verify cell purity. The pure populations of CD11b-positive cells from naïve and tumor-bearing WT and TLR2 mice were then used for investigating gene expression changes in MT1-MMP by real-time quantitative (q)PCR.

Generation of EGFP-GL261 and mCherry-GL261 Cells

GL261 glioma cells were transfected with the pEGFP-N1 vector for stable expression of enhanced green fluorescent protein (EGFP; Clonetech) using Lipofectamine 2000 transfection reagent (Invitrogen) according to the manufacturer's instructions. The pEGFP-N1 vector contains the human cytomegalovirus promoter, which drives high-level expression of the EGFP in transfected cells. Using the Genetecin-G418 selection method (600 μg/mL; Gibco), stably transfected clones of GL261 cells were established.

Viable cells with bright fluorescence were selected by fluorescence activated cell sorting analysis. These cells were used for glioma inoculation in organotypic brain slices. On the day of injection, 90%–95% of cells were fluorescent.

The mCherry-GL261 cell line was generated by transfecting OmicsLink nontargeted short hairpin RNA tagged with mCherry (GeneCopoeia) according to the manufacturer's instructions. Transfected GL261 cells were then selected by treating with 5 μg/mL puromycin and used further for in vivo tumor implantation experiments. The mCherry-GL261 cell line was chosen over EGFP-GL261 cells for in vivo studies due to higher stability of its fluorescence signal.

Preparation of Glioma-conditioned Medium

GL261 cells were seeded at a density of 1×10^6 cells in 75 cm^2 tissue culture flasks and grown to 80% confluence. Cells were then replenished with fresh complete growth medium, which was left on the cells for 16–18 h before being harvested. The conditioned medium was collected, briefly centrifuged to remove cell debris, filtered using a 0.2-μm filter (Sartorius Stedim Biotech), and used for all further experiments.

TLR Subtype-specific Ligands

Different TLR subtype-specific agonists and TLR2-specific agonists (Cayla-Invivogen) were used to investigate MT1-MMP gene expression in microglial cells from WT mice. The following concentrations of agonists were used based on the maximal effects observed in cytokine/chemokine induction assays: TLR1/2 agonist, palmitoyl-3-cysteine-serine-lysine-4 (Pam_3CSK_4; 10 ng/mL); TLR3 agonist, polyinosinic:polycytidylic acid (poly(I:C)) (10 μg/mL); TLR4 agonist, lipopolysaccharide (LPS; 100 ng/mL); TLR5 agonist, flagellin (500 ng/mL); TLR2/6 agonist, macrophage-activating lipopeptide (MALP)2 (500 ng/mL); TLR7/8 agonist, polyuridine (polyU; 5 μg/mL); and TLR2 agonists, heat-killed Listeria monocytogene (HKLM; 1×10^5 cells/mL) and *Porphyromonas gingivalis* (PG)–LPS (1 μg/mL). Microglial cells were stimulated with these ligands for 6 h to analyze changes in MT1-MMP gene expression by real-time qPCR.

Real-time qPCR and Western Blot

Total RNA was isolated from microglia obtained from WT and TLR1, 2, 6, 7, and 9 KO mice using the Invitrap Spin Universal RNA mini kit (Invitek); quality and yield were determined by NanoDrop 1000 (PeqLab Biotechnologie). Complementary DNA was synthesized using 100–250 ng total RNA by the extension of oligodeoxythymidine$_{12-18}$ primers (0.5 μg/μL) with 200 U/μL SuperScript II reverse transcriptase (Invitrogen). Gene amplification was done in triplicate using SYBR Green PCR mix (Roche Diagnostics) with the following PCR conditions for MT1-MMP: 95°C for 2 min, 95°C for 15 s, 55°C for 15 s, and 68°C for 20 s for 35 cycles using the Realplex Mastercycler (Eppendorf); for TLR2 and IL-10: 95°C for 10 min, 95°C for 15 s, and 60°C for 60 s for 40 cycles using the 7500 Fast real-time qPCR System (Applied Biosystems). Sequences of primers used were: sense 5′-GTGCCCTATGCCTACATCCG-3′, anti-sense 5′-CAGCCACCAAGAAGATGTCA-3′ (MT1-MMP); sense 5′- CCCTGTGCCACCATTTCC-3′, anti-sense 5′- CCACGCCCACATCATTCTC-3′ (TLR2); sense 5′-GCTCTTACTGACTGGCATGAG-3′, anti-sense 5′-CG CAGCTCTAGGAGCATGTG-3′ (IL-10), sense 5′-CCCT GAAGTACCCCATTGAA-3′, anti-sense 5′-GTGGACAG TGAGGCCAAGAT'-3′ (β-actin). Changes in MT1-MMP or TLR2 gene expressions were analyzed by the comparative $2^{(-\Delta\Delta Ct)}$ method relative to β-actin gene expression levels. The same PCR conditions were used for investigating MT1-MMP IL-10 gene expression changes in CD11b-positive cells isolated from naïve and tumor-bearing WT and TLR2 KO mice. Total RNA from 4 independent biological experiments were used for determining mean fold change differences ± SEM in MT1-MMP gene expression.

Whole-cell protein extracts were prepared from glioma conditioned medium (GCM)–treated microglia of WT and TLR2 KO mice using radioimmunoprecipitation assay lysis buffer (Sigma-Aldrich) containing EDTA-free protease inhibitor cocktail tablets (Roche Diagnostics). Protein concentration was determined by a bicinchoninic acid protein assay kit (Thermo Fisher Scientific), and 20 μg of total protein of each sample was resolved on a 10% sodium dodecyl sulfate–polyacrylamide gel electrophoresis gel, followed by wet transfer of resolved proteins onto a polyvinylidene difluoride membrane (Amersham GE). The membranes were blocked in 5% bovine serum albumin (Carl-Roth) in phosphate buffered saline (PBS)–Tween 20, pH 7.4, followed by overnight incubation at 4°C with rabbit anti–MT1-MMP antibody (1:1000; Epitomics). The membranes were incubated with a secondary anti-rabbit horseradish peroxidase antibody (1:2000; Cell Signaling Technology), developed with the SuperSignal West Pico Chemiluminescence substrate kit (Thermo Fisher Scientific) and the signal detected by a Molecular Imager Gel Doc XR system (Bio-Rad Laboratories). Differences in MT1-MMP protein expression between WT and TLR2 KO microglia were densitometrically analyzed using ImageJ software (National Institutes of Health).

Flow Cytometry

Primary neonatal microglial cells from WT or TLR2 KO mice were incubated with isotype control (immunoglobulin G2a) or anti-mouse CD282/TLR2-phycoerythrin antibody (clone mT2.7, eBioscience), and the expression of TLR2 was determined by an LSR II flow cytometer (BD Biosciences). Data analysis was done using FlowJo software (Treestar).

Chemotaxis Boyden Chamber Assay

To determine whether TLR2 agonists induced migration in microglia, chemotaxis experiments were performed as

described previously.[37] The TLR2 agonists Pam_3CSK_4 (10 ng/mL), HKLM (1×10^5 cells/mL), and PG-LPS (1 μg/mL) in serum-free DMEM were pipetted into the lower compartments of a 48-well microchemotaxis chamber (Neuroprobe), which was then assembled with an 8-μm pore polycarbonate membrane (Neuroprobe). As a positive control, we used 100 μM adenosine-5′-triphosphate (ATP; Sigma Aldrich). Primary microglial cells from WT mice in suspension (1000 cells/μL) were added to the upper compartment of the chamber. After 6 h incubation at 37°C/5% CO_2, the membrane was fixed and stained with the Diff Quik staining kit (Medion Diagnostics), dried, and mounted on a glass slide. Nonmigrated cells on the upper side of the membrane were wiped off with a cotton swab. Microglial cell migration was determined by counting 4 representative fields per well from 3 wells per experiment. The data represent mean ± SEM from 3 independent experiments.

Organotypic Brain Slice Model and Tumor Inoculation

Brain slices were derived from 16-day-old WT and TLR2 KO mice. Mice were decapitated and brains were removed within 2–3 min and placed in ice-cold PBS under sterile conditions. The forebrain was dissected from the brainstem, glued with cyanoacrylate glue (Uhu) onto a magnetic block, and cut in the coronal plane into 250-μm sections with a vibratome (Leica VT1000S). Brain slices were transferred into cell culture inserts of 0.4-μm pore size (Becton Dickinson) that were fitted into wells of a 6-well plate. Thereafter, 1 mL of culture medium containing DMEM (Gibco) supplemented with 10% heat inactivated fetal calf serum (FCS; Invitrogen), 0.2 mM glutamine, 100 U/mL penicillin, and 100 mg/mL streptomycin (all from Gibco) was added into each well and the brain slices were incubated in the inserts at an air/medium interface. After overnight equilibration, the culture medium was exchanged for cultivation medium that contained 25% heat-inactivated FCS, 50 mM sodium bicarbonate, 2% glutamine, 25% Hank's Balanced Salt Solution, 1 mg/mL insulin (all from Gibco), 2.46 mg/mL glucose (Braun Melsungen), 0.8 mg/mL vitamin C (Sigma-Aldrich), 100 U/mL penicillin, 100 mg/mL streptomycin (Gibco), and 5 mM Tris in DMEM (Gibco).

Selective depletion of microglia in organotypic brain slices (OBS) was achieved following a previously established protocol[38] by adding liposome-encapsulated clodronate diluted with culture medium (1:10) to the slices. The slices were left with clodronate for 24 h, which led to a 90% ablation of microglia. After 24 h, the culture medium containing clodronate was replaced by fresh cultivation medium and slices were left undisturbed for 72 h. After 3 days, slices from WT and TLR2 KO mice were inoculated with EGFP-GL261 cells to investigate the effect of microglia depletion on tumor growth.

Five thousand EGFP-GL261 glioma cells in a volume of 0.1 μL were inoculated into brain slices of WT and TLR2 KO mice using a 1-μL syringe mounted on a micromanipulator. This device allowed placement of the tip of the syringe consistently at the same defined region on the slice surface. An injection canal was formed that reached 150 μm deep into the 250-μm-thick slice. The needle was then retracted by 50 μm, leaving a cavity of ~50 μm in length. The cell suspension was injected slowly into this canal in the slices. To ensure identical experimental conditions, glioma cells were always inoculated into the same area of the slices, into the globus pallidus in the cortex. Directly after glioma injection, tumor cells remained at the inoculation site. Careful control of the injection procedure ensured that no cells spilled onto the surface of the slices, which could migrate over the surface rather than invade through the tissue.

In vivo Glioma Implantation

WT and TLR2 KO mice were used for all in vivo studies to investigate MT1-MMP expression by immunohistochemistry, tumor expansion, and survival rates. Briefly, mice were anesthetized, immobilized, and mounted onto a stereotactic head holder (David Kopf Instruments) in the flat-skull position. After skin incision 1 mm anterior and 1.5 mm lateral to the bregma, the skull was carefully drilled with a 20G needle tip. A 1-μL syringe with a blunt tip (Mikroliterspritze 7001N) was inserted to a depth of 4 mm and retracted to a depth of 3 mm from the dural surface into the right caudate putamen. Over 2 min, 1 μL (2×10^4 cells/μL) of mCherry-GL261 glioma cell suspension was slowly injected into the brain. The needle was then carefully retracted from the injection canal and the skin was sutured with a surgical sewing cone (Johnson & Johnson International). After surgery, the mice were kept warm until awake and their postoperative condition was monitored daily.

Immunohistochemical Detection of MT1-MMP

All immunohistochemical stainings were performed on 40-μm-thick free-floating brain sections from WT and TLR2 KO mice. Sections were washed with PBS-Tween 20, pH 7.4, followed by antigen retrieval using sodium citrate buffer, pH 6, at 95°C for 20 min in a water bath. Nonspecific staining in sections was blocked using 3% donkey serum in PBS-Tween 20 for 1 h at room temperature followed by overnight incubation at 4°C with primary antibodies for goat anti-Iba1 (1:500; Abcam) and rabbit anti–MT1-MMP (1:200; Epitomics). MT1-MMP expression was detected using anti-rabbit biotin streptavidin peroxidase–conjugated immunoglobulin G (1:200; Jackson Immunoresearch) and streptavidin-conjugated Cy5 (1:200; Jackson Immunoresearch). Iba1 was detected using the secondary antibody anti-goat DyLight 488 (1:200; Jackson Immunoresearch). Nuclear staining was visualized using 4′,6′-diamidino-2-phenylindole (1:1000; Sigma-Aldrich). The GL261 glioma cells were identified by red fluorescence of the mCherry construct.

In vivo Assessment of Glioma Expansion

Glioma growth was assessed in vivo in WT and TLR2 KO mice by MRI. Mice were anesthetized with 2.8% isoflurane in an oxygen/air mixture (2:1) with a flow rate of 750 mL/min and maintained at 1.5%–2% for the entire experiment as described before. Respiration rate and body temperature were continuously monitored by a Model 1025 system (SA Instruments). Body temperature was maintained at 37°C throughout the experiment using a heated circulating water system.

The 2 groups of WT and TLR2 KO mice ($n = 11$ per group) were imaged 21 days after intracerebral inoculation of GL261 cells. All MR imaging was performed on a horizontal bore 9.4 T small animal MRI system (Biospec 94/20, Bruker Biospin) using a cryogenically cooled H-probe head (Z106543, 400 MHz, Bruker BioSpin MRI). T_2-weighted images (rapid acquisition with relaxation enhancement [RARE], effective echo time = 60 ms; repetition time = 3268 ms; RARE factor = 12) were acquired with the same slice geometry (field of view = 18 mm, matrix size = 350 × 350, slice thickness = 270 μm, in-plane spatial resolution = 51 μm), 21 coronal slices covering a brain region of 5.67 mm starting at the frontal end of the cerebral cortex (approx bregma 3.56 to −2.11 mm).[39] The T_2 contrast was optimized beforehand in pilot experiments to achieve good tumor delineation. The total experimental time, including animal preparation, was ~70 min per animal. Tumor volumes were calculated by manual segmentation using the software *mipav* (http://mipav.cit.nih.gov). A region of interest (ROI) following the tumor borders was drawn with exclusion of the needle path (stemming from the tumor cell injection) in the T_2-weighted images. The whole tumor volume was calculated by adding up the voxel volumes within the ROIs of all image slices.

Unbiased Stereology for Tumor Volume Estimation

Mice were anesthetized with Narcoren 14 days after tumor inoculation, brains perfused and fixed, and resulting brain slices were subsequently used to analyze tumor expansion in vivo. The tumor volume in hematoxylin and eosin (H&E) stained brain slices of glioma-bearing WT and TLR2 KO mice ($n = 8$ per group) was quantified according to the Cavalieri principle by determining tumor area in every 12th 40-μm-thick brain slice and then multiplying this area by the factor 12 × 40 μm.[40]

Analysis of Survival

To investigate a possible effect of TLR2 on survival in tumor-bearing mice, adult female WT and TLR2 KO mice ($n = 15$ per group) were intracranially implanted with gliomas. Briefly, 2×10^4 cells/μL of GL261 glioma cell suspension was slowly injected into the brain as stated previously. Analysis of cumulative mean survival time by Kaplan–Meier plots in tumor-implanted WT and TLR2 KO mice was based on the endpoint event (mice alive after a certain time). The endpoint was 36 days, the longest time of survival of tumor-implanted TLR2 KO mice.

Image Acquisition and Processing

Images of immunohistochemically stained brain slices were taken using a Leica confocal microscope with a 40X oil objective. Fluorescent images were taken from at least 3 random fields of interest (microglia in the tumor periphery) from WT and TLR2 KO mice. Cells positively labeled for Iba1 in these images were counted using ImageJ software.

REMBRANDT Data

The microarray gene expression and clinical data for *TLR2* were acquired from the Repository of Molecular Brain Neoplasia Data (REMBRANDT; http://rembrandt.nci.nih.gov) on June 7, 2012. Kaplan–Meier survival curves for differential TLR2 gene expression were plotted for 454 glioma patient samples versus 28 nontumor cases. A log-rank *P*-value determined significant differences in survival between the upregulated, downregulated, and intermediate samples. A 2-fold difference from the mean expression level within a given data set was defined as upregulation (>2-fold) or downregulation (<2-fold).

Statistical Analyses

All analyses were performed using SPSS software and Microsoft Excel 2007. Statistically significant changes in MT1-MMP gene expression were determined by the Mann–Whitney *U*-test and Student's *t*-test. Differences in tumor volumes between WT and TLR2 KO mice were estimated using the unpaired Wilcoxon rank-sum test. The Kaplan–Meier method was used for assessing cumulative survival times, and significant differences between WT and TLR2 KO mice were compared by the log-rank test. Statistical significance was determined at $P < .05$ (*) and $P < .01$ (**), while n.s. implied a nonsignificant *P*-value.

Results

TLR2-deficient Mice Show Reduced Glioma Growth and MT1-MMP Expression and Enhanced Survival Rate

To investigate whether ablation of the TLR2 gene locus interfered with tumor expansion in vivo, we inoculated GL261 cells into WT and TLR2 KO mice (for knockout efficiency, see Supplementary materials, Fig. S1) and measured tumor volumes. Tumor volumes were calculated by 2 different approaches—firstly by unbiased stereological estimation (Cavalieri method) after tumor-implanted mice were sacrificed, and secondly by MRI of WT and TLR2 KO tumor-bearing mice. Tumor volumes were significantly reduced in TLR2 KO mice compared with WT mice in both methods of evaluation. The H&E stained

image in Fig. 1A represents the gross morphology of glioma in WT and TLR2 KO mice as assessed by the Cavalieri method. After 2 weeks of tumor implantation, the tumor volume in TLR2 KO mice was significantly reduced to 34% ($P = .031$) relative to the tumor volume in WT mice. Figure 1B represents a T_2-weighted MR image of a hyperintense tumor (delineated by dotted black circle) of WT and TLR2 KO mice. Here, the relative tumor volume was significantly reduced to 46.4% ($P = .018$) in the TLR2 KO mice compared with that in the WT mice as determined 21 days after glioma implantation.

To investigate whether TLR2 mediates glioma-induced upregulation of microglial MT1-MMP, we examined the expression of MT1-MMP in WT and TLR2 KO mice inoculated with glioma cells. After 2 weeks of tumor growth, brain tissue was analyzed by immunohistochemistry for MT1-MMP expression. GL261 glioma cells were identified by stable expression of mCherry, while GAMs were identified by immunolabeling with the microglia/macrophage-specific antibody Iba1. We observed an increase in MT1-MMP immunoreactivity in GAMs closely associated with the invasive edge of the glioma tumor in WT mice (Fig. 1C upper panel), whereas in TLR2 KO mice, the immunoreactivity of MT1-MMP in GAMs was decreased (Fig. 1C lower panel). GAMs closely associated with the tumor margin in WT mice had an ameboid morphology, while GAMs in TLR2 KO mice appeared more ramified (Fig. 1C insets). Moreover, we also examined whether the TLR2 KO condition caused a reduction in GAM density at the invasive edge of the glioma. There was only a modest reduction in GAM density in the TLR2 KO mice compared with the WT mice (Fig. 1C), indicating that TLR2 is not the only signaling pathway responsible for attraction of microglia/brain macrophages to the tumor edge.

Since the in vivo fluorescent quantification of MT1-MMP in brain slices from tumor-implanted WT and TLR2 KO mice was difficult, we determined MT1-MMP gene expression in microglia/brain macrophages freshly isolated from naïve and glioma-bearing WT and TLR2 KO mice by real-time qPCR (Fig. 1D). MT1-MMP gene expression in GAMs from WT mice was increased 4.08-fold (± 0.204; $P = .002$) relative to that in GAMs from naïve microglia from WT mice. In GAMs derived from TLR2 KO mice, MT1-MMP gene expression was 2.19-fold (± 0.26; $P = .02$) upregulated relative to its expression in naïve microglia from TLR2 KO mice. Overall, MT1-MMP gene expression in GAMs from TLR2 KO mice was significantly lower ($P = .045$) than that in GAMs from WT mice. To assess whether MT1-MMP had any effect on specific M2 type macrophage markers in glioma-associated and naïve microglia, we evaluated the gene expression of the classic M2 macrophage marker IL-10 by real-time qPCR with the same samples used above. We could not observe any significant differences in IL-10 gene expression between the naïve microglia and GAMs, as also previously reported by Gabrusiewicz et al.[41] Furthermore, there was no difference in IL-10 gene expression in the TLR2 KO GAMs compared with the WT GAMs (see Supplementary material, Fig. S4).

We also investigated survival rates of glioma-bearing WT and TLR2 KO mice. As seen in Fig. 1E, deletion of the TLR2 gene locus led to significantly increased survival rate ($P = .006$) in TLR2 KO mice compared with tumor-bearing WT mice, thereby suggesting that TLR2 expression relates to poor prognosis in mice models of experimental gliomas.

TLR2 Deletion and Microglia Ablation Interfere With Glioma Growth Ex vivo

Tumor expansion can be well documented in microglia-containing or -depleted organotypic brain slices. Microglia in brain slices were depleted using liposome-encapsulated clodronate[11] followed by inoculation of EGFP-GL261 glioma cells into the slices 2 days after clodronate treatment (Fig. 2A). We analyzed the area occupied by glioma cells 5 days later (Fig. 2B). Tumor size in microglia-depleted brain slices from WT mice was significantly reduced to 48% ($P = .0031$) relative to tumor size in microglia-containing brain slices from WT mice. The average tumor size in microglia-containing slices from TLR2 KO mice was reduced to 46% ($P = .026$) relative to tumor size in brain slices from WT mice. The ablation of microglia in brain slices from TLR2 KO mice led to a further reduction of tumor size to 28% ($P = .022$) relative to that in microglia-containing brain slices of TLR2 KO mice. These results indicate that microglia-induced glioma expansion is mediated by TLR2-dependent and -independent mechanisms.

To test whether other TLR(s) apart from TLR2 were involved in glioma growth ex vivo, we prepared organotypic brain slices from WT and TLR7 KO mice (p16 in age). In slices from both types of mice, tumors were significantly smaller when microglial cells were depleted ($P < .001$ in WT and $P < .01$ in TLR7 KO mice; Supplementary material, Fig. S2A and B), but there was no difference in the tumor sizes between microglia-containing WT and TLR7 KO groups ($P = .45$), hence indicating that TLR7 is dispensable for glioma growth.

TLR2 Ligands Mimic the Effect of GCM on Microglial MT1-MMP Gene Expression but Do Not Alter Microglial Cell Migration In vitro

To investigate whether MT1-MMP gene expression in microglia could be induced by distinct TLRs, we stimulated primary microglia from WT mice with both specific TLR ligands and GCM for 6 h and analyzed changes in MT1-MMP gene expression by real-time qPCR (Fig. 3A). The TLR1/2 ligand Pam_3CSK_4 induced a 3-fold (± 0.075; $P = .0076$) increase in MT1-MMP gene expression relative to the untreated control, while in the GCM-stimulated microglia there was a 2.5-fold (± 0.07; $P = .035$) increase in MT1-MMP gene expression. There was no significant change induced by the TLR3 agonist poly(I:C), with a 1.4-fold change (± 0.051; $P = .082$) in MT1-MMP gene expression relative to the WT control. The TLR4 ligand LPS induced a 1.8-fold change (± 0.055; $P = .067$), while the TLR2/6 agonist

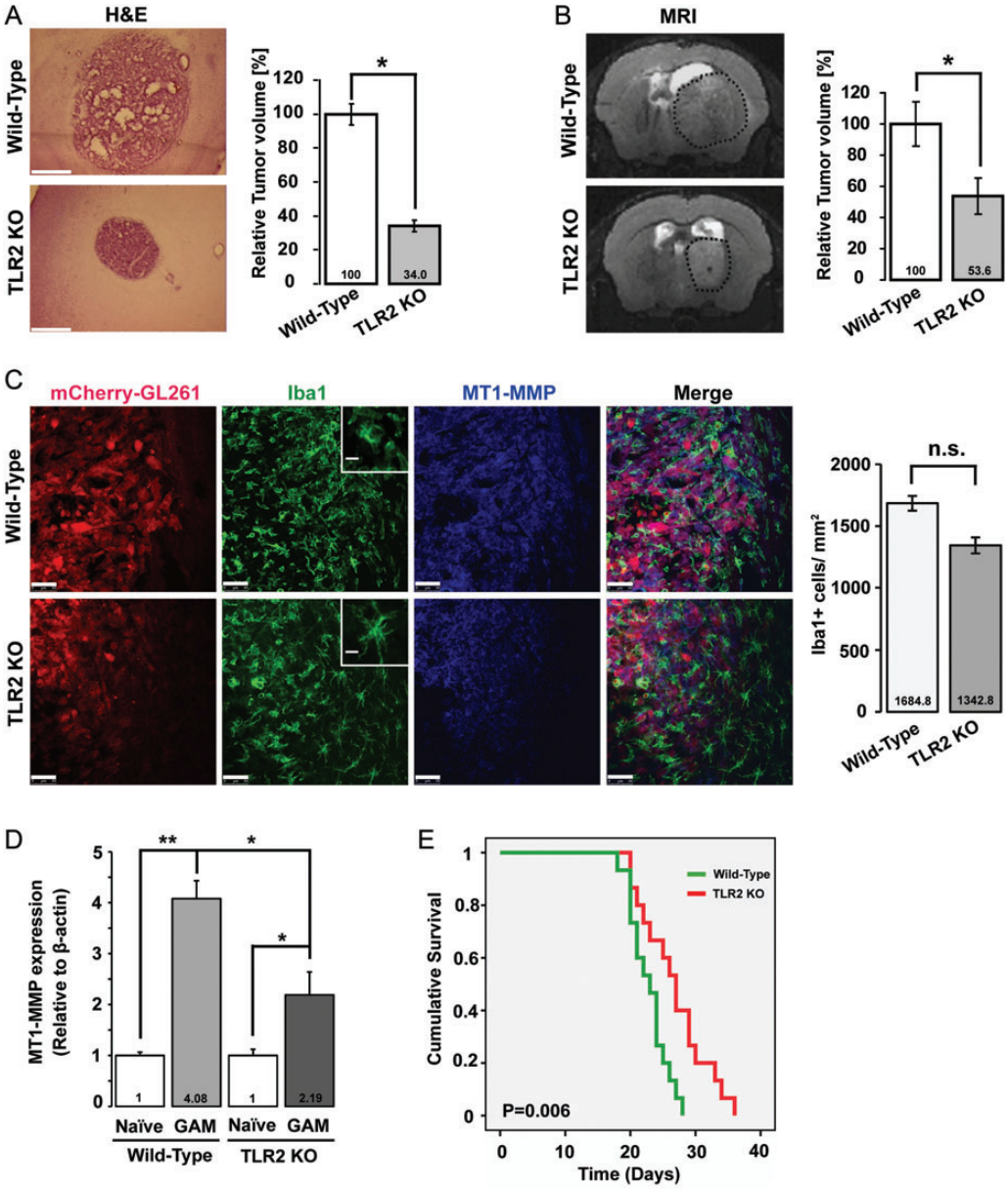

Fig. 1. Absence of TLR2 results in reduced tumor expansion, decrease in MT1-MMP expression, and increased survival. (A) Deletion of the TLR2 gene locus impacts tumor expansion in vivo. Mouse GL261 cells were i.c. implanted into WT and TLR2 KO mice. The images on the left show H&E stained slices from glioma-bearing WT and TLR2 KO mice. On the right, the relative tumor volume in WT versus TLR2 KO animals was evaluated based on unbiased stereology. Scale bar is 500 μm . (B) A representative MRI T_2-weighted image of a hyperintense tumor (delineated by dotted black circle) from WT and TLR2 KO mice. The relative tumor volume in WT and TLR2 KO mice is shown on the right. Statistical significance was analyzed by Wilcoxon's rank-sum test and significance was taken at $P < .05$(*) and $P < .01$(**). The significance is indicated in the bars. (C) Slices from glioma inoculated WT and TLR2 KO mice were immunohistologically labeled. Glioma cells were identified by stable expression of mCherry, microglia/brain macrophages by the expression of Iba1, and MT1-MMP by immunolabeling. The insets illustrate the morphology of GAMs in WT and TLR2 KO mice. While WT GAMs had ameboid morphology, GAMs in the TLR2 KO mouse were more ramified. Scale bars are 50 μm and 10 μm (for insets). The GAM cell density near the invasive edge of glioma is shown in the graph on the right. (D) WT and TLR2 KO mice were i.c. implanted with glioma tumors, and GAMs were isolated 14 days after glioma cell injection. Naïve tumor-free brain was used as a control. Data were collected from 3 different mice in each group. Differences in MT1-MMP gene expression were analyzed by $2^{(-\Delta\Delta CT)}$ method. MT1-MMP gene expression in WT GAMs is 4.08-fold upregulated (± 0.204, $P = .002$) compared with WT naïve microglia, while in TLR2 KO GAMs, MT1-MMP gene expression was 2.19-fold upregulated (± 0.26, $P = .02$). MT1-MMP gene expression in TLR2 KO GAMs is significantly decreased compared with WT GAMs ($P = .045$). Statistical significance was analyzed by Student's *t*-test and significance was taken at $P < .05$(*) and $P < .01$(**). (E) The Kaplan–Meier curves represent the cumulative survival of WT and TLR2 KO mice after glioma cell injection ($P = .006$).

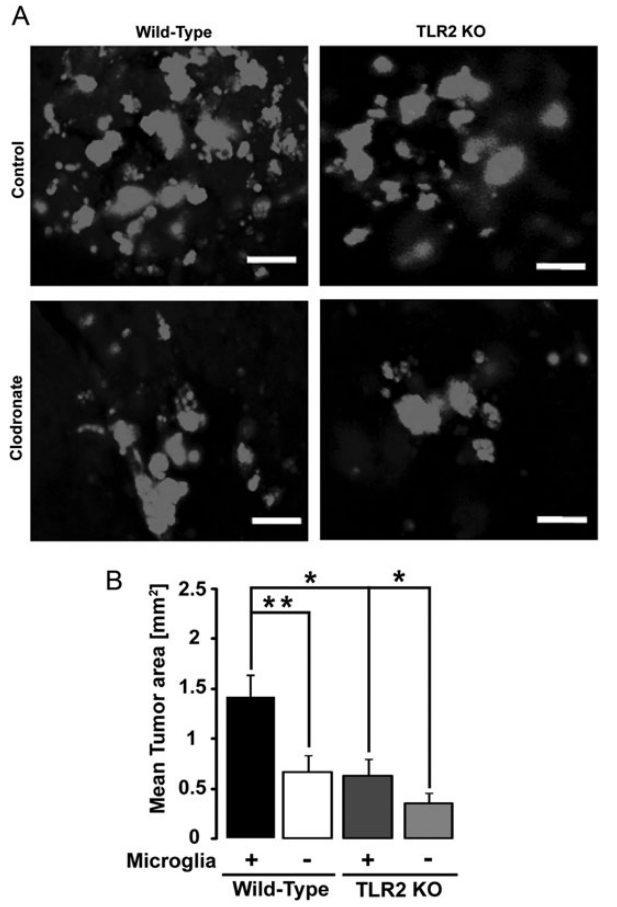

Fig. 2. TLR2 interferes with glioma growth ex vivo. TLR2 expressed by microglia contributes to glioma expansion in organotypic brain slices. Brain slices from 16-day-old WT and TLR2 KO mice were implanted with 5000 EGFP-GL261 glioma cells, and the area occupied by glioma cells was measured after 5 days. (A) The fluorescence micrograph of EGFP-labeled glioma cells in both microglia-containing and -depleted brain slices for WT (left) and TLR2 KO (right) mice. Scale bar is 10 μM. (B) Tumor area was quantified in both microglia-containing (+) and -depleted (−) slices from WT and TLR2 KO mice. Statistical significance was analyzed by Wilcoxon's rank-sum test and significance was taken at $P < .05$(*) and $P < .01$(**).

MALP2 caused a modest but significant 1.7-fold (± 0.096; $P = .04$) upregulation in MT1-MMP gene expression, compared with untreated control. The TLR5 agonist flagellin (1-fold; $P = .098$) and TLR7/8-specific polyU (0.7-fold; $P = .105$) did not cause any significant changes in MT1-MMP gene expression.

To analyze whether MT1-MMP gene expression changes were specific to TLR2 activation, primary microglia from WT mice were further stimulated with known TLR2 agonists such as PG-LPS from *P. gingivalis* and HKLM for 6 h. A robust induction of MT1-MMP gene expression with both agonists was observed (GCM: 4.4 ± 1.5, $P = .046$; Pam_3CSK_4: 5.4 ± 0.9, $P = .033$; HKLM: 6.2 ± 0.4, $P = .023$; PG-LPS: 4.0 ± 0.7,

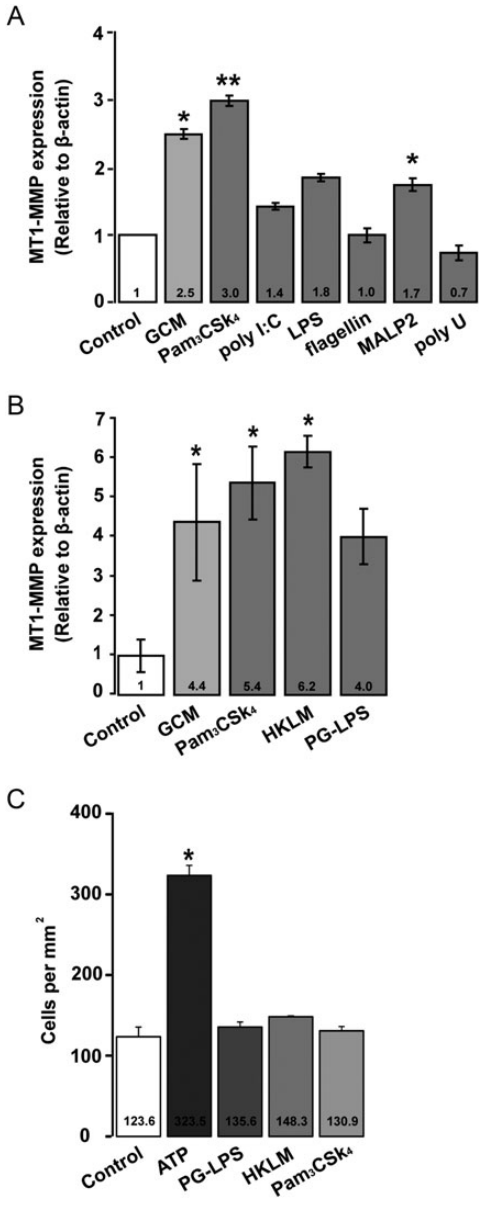

Fig. 3. TLR agonists differentially regulate microglial MT1-MMP gene expression but do not alter chemotaxis in microglia. (A) The influence of subtype-specific ligands of TLRs on MT1-MMP gene expression was determined in primary microglia from WT mice. Microglia were stimulated with agonists and GCM for 6 h and differences in MT1-MMP gene expression were analyzed by the $2^{(-\Delta\Delta CT)}$ method. (B) Microglia were stimulated with TLR2-specific agonists PG-LPS and HKLM for 6 h, which showed a significant induction of MT1-MMP gene expression. Statistical significance was analyzed by Mann–Whitney *U*-test and significance was taken at $P < .05$(*) and $P < .01$(**). (C) The impact of the TLR2 agonists Pam_3CSK_4, PG-LPS, and HKLM on microglial chemotaxis was determined in a 48-well microchemotaxis chamber. ATP was used as a positive control. No significant differences were observed in microglia migration between the control group (only DMEM) and TLR2 agonists group after 6 h of incubation.

$P = .061$; Fig. 3B). These results indicate that TLR2 is the major TLR mediating changes in MT1-MMP gene expression in microglial cells.

To investigate whether TLR2-specific ligands promote migratory activity in microglia, we studied chemoattraction using the Boyden chamber chemotaxis assay. None of the TLR2-specific agonists (ie, Pam_3CSK_4, PG-LPS, and HKLM) stimulated migration in primary microglial cells within 6 h compared with control conditions. ATP served as a positive control and triggered a high rate of chemotaxis in microglia (Fig. 3C).

Costimulation of TLR1/TLR6 Is Required for Inducing TLR2-dependent MT1-MMP Gene Expression in Microglia

TLR2 signaling can be mediated by heterodimerization with TLR1 and TLR6. To determine the contribution of TLR1 and TLR6 to glioma-induced MT1-MMP gene expression in microglia, we stimulated microglial cells from WT, TLR1, and TLR6 KO mice with GCM. Microglial cells were incubated for 6 h with GCM, and MT1-MMP gene expression was analyzed by real-time qPCR. Indeed, absence of TLR2 did not lead to an increase in MT1-MMP gene expression (Fig. 4A), whereas in WT microglia used as controls, we detected a 2.51-fold ($P = .027$) increase in MT1-MMP gene expression. In microglia from TLR1 and TLR6 KO mice, we observed a 1.7-fold ($P = .041$) and a 1.3-fold ($P = .023$) change, respectively, in MT1-MMP gene expression, thus lower compared with microglial cells from WT control mice (Fig. 4B and C).

We further stimulated microglial cells from TLR7 and TLR9 KO mice with GCM for 6 h and observed a robust increase in MT1-MMP gene expression (4.8-fold, $P = .021$ in TLR7 KO and 3.05-fold, $P = .076$ in TLR9 KO group) as also seen in microglia from WT mice (Fig. 4D and E). Consistent with our data from real-time qPCR, we also observed that TLR2 is needed to induce MT1-MMP protein expression in GCM-stimulated microglia as observed by immunoblotting (Fig. 4F).

These results support our in vivo data that TLR2 in GAMs is required to mediate microglial MT1-MMP gene and protein expressions and identified TLR1 and TLR6 as potential heterodimeric partners of TLR2 in this process.

TLR2 *Is Highly Expressed in Human Gliomas and Its Expression Inversely Correlates With Patient Survival*

We used REMBRANDT to analyze whether high *TLR2* expression correlated with clinical data from human glioma patients. Indeed, *TLR2* was highly expressed in all gliomas ($n = 454$) compared with 28 cases of nontumor tissue (Supplementary material, Fig. S3A). Comparing the probability of survival in all glioma cases, patients with upregulated *TLR2* revealed a lower survival rate (Supplementary material, Fig. S3B). This may indicate that patients with high *TLR2* expression usually suffer from a higher-grade glioma and that patients with lower *TLR2* expression have a lower-grade glioma. Moreover, even survival rates within a homogeneous group of tumors (ie, astrocytomas) correlated with the expression of *TLR2*. Patients with high *TLR2* expression levels presented with reduced survival compared with patients having lower *TLR2* expression (Supplementary material, Fig. S3C).

Discussion

Our present study highlights the importance of microglial TLR2 in inducing MT1-MMP gene and protein expressions for promoting glioma expansion and progression in an experimental mouse model of glioma. In a previous study, we observed that the TLR adaptor protein MyD88 was required for upregulating microglial MT1-MMP gene and protein expression induced by GCM.[12] MyD88 is involved in signaling by TLRs 1, 2, 4, 5, 6, 7, 8, and 9, but not in TLR3 signaling.[42] Microglial cells represent the predominant TLR-expressing cells in the CNS.[43] We used TLR subtype-specific agonists to stimulate different TLRs and analyzed the gene expression of MT1-MMP as a most relevant read-out. We found that the TLR1/2 agonist Pam_3CSK_4 mimicked the response to GCM by inducing a 3-fold upregulation in MT1-MMP gene expression in primary microglia after 6 h. The involvement of TLR2 was further confirmed by the effect of TLR2-specific agonists, namely PG-LPS and HKLM, on microglial MT1-MMP gene expression. Agonists of other TLR subtypes like LPS (TLR4), MALP2 (TLR2/6), flagellin (TLR5), and polyU (TLRs 7/8) induced only a minor or no change in MT1-MMP gene expression. The involvement of TLR2 in mediating the protumorigenic effect of GAMs was confirmed through our studies on TLR2-deficient mice. TLR2 KO mice inoculated with glioma cells had smaller tumors analyzed after 2 weeks of tumor implantation and showed better survival rates in comparison with tumor-bearing WT mice. Furthermore, there was a marked reduction in both MT1-MMP mRNA expression and immunolabeling in glioma-associated microglia/brain macrophages from TLR2 KO mice compared with WT mice, but only a modest reduction in intra- and peritumoral microglia density. Consistently, our in vitro data indicated that TLR2 signaling did not mediate chemotaxis in microglia. Altogether, our data point out that TLR2 signaling specifically mediates MT1-MMP expression, but not tumor tropism in microglia.

Our studies on organotypic brain slices injected with glioma cells further confirmed that TLR2 exerts a significant effect on tumor expansion. In slices obtained from TLR2 KO mice, the glioma cells occupied a smaller area compared with slices from WT mice. When we compared glioma expansion in microglia-containing or microglia-depleted brain slices from TLR2 KO, we found that TLR2 was a major but not the sole signaling pathway controlling microglia-mediated glioma expansion. Data from other TLR KO mice, such as TLR7 KO mice, revealed that glioma tumor expansion ex vivo specifically required TLR2 (see Supplementary material, Fig. S2).

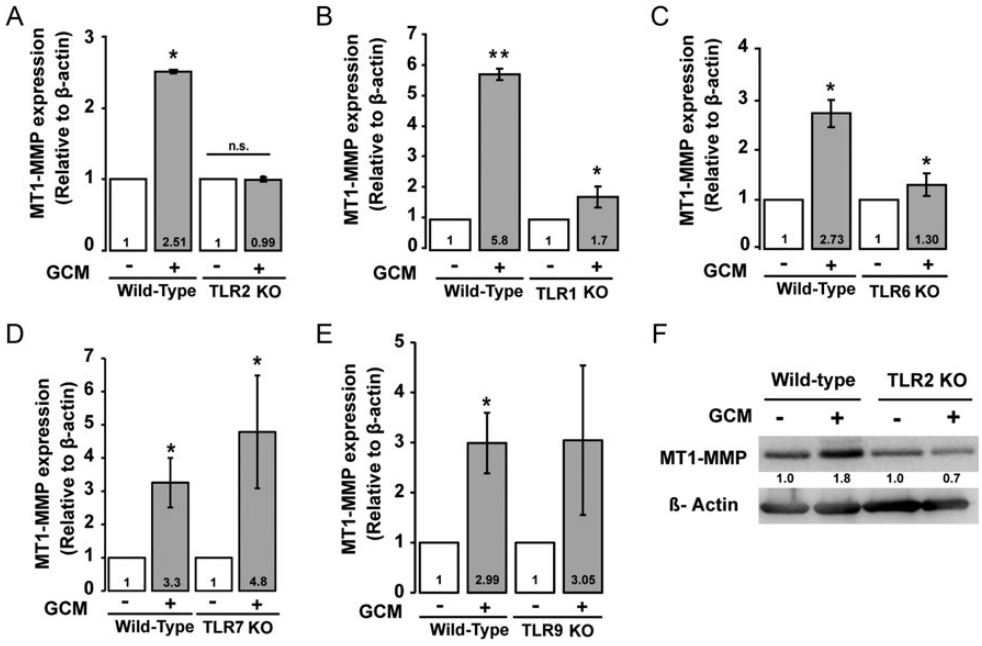

Fig. 4. MT1-MMP gene expression induced by GCM in microglia from different TLR-deficient mice. (A) Microglia from WT and TLR2 KO mice were stimulated with GCM for 6 h and MT1-MMP gene expression was analyzed by real-time qPCR and compared with an unstimulated control. Similarly, MT1-MMP gene expression was analyzed in (B) TLR1, (C) TLR6, (D) TLR7, and (E) TLR9 KO mice. (F) A representative western blot image of MT1-MMP protein expression in GCM-stimulated microglial cells from TLR2 KO and WT control. MT1-MMP expression is reduced in TLR2 KO microglia, as seen in the quantification of the western blot (values indicated below the bands).

TLRs are considered as receptors binding to various nonself signals such as bacterial cell wall components or viral products. There is, however, increasing evidence that TLRs can also be activated by endogenous host-derived ligands.[44] Our cell culture studies showed that glioma cells release still unidentified soluble factor(s) that activate TLR2 in GAM cells. Gliomas constitutively release heat-shock proteins, high-mobility group box (HMGB)1 protein, and hyaluronan,[45–48] and these factors recognize and interact with various TLRs, in particular TLRs 2 and 4. Moreover, TLRs can also be activated in vivo by factors liberated due to sterile inflammation, hypoxia, or necrosis, which are common pathologic events associated with malignant, invasive, or dying glioma cells. Curtain et al.[47] induced glioma cell death through cytotoxic therapies. They showed that the dying glioma cells released HMGB1 and thereby recruited myeloid dendritic cells through TLR2 signaling. These recruited dendritic cells led to tumor regression. However, in our study, we had no cytotoxically induced dying glioma cells and focused rather on elucidating the molecular mechanism of the protumorigenic impact of microglial TLR2 on glioma expansion and infiltration through MT1-MMP. Additionally, TLR signaling can be activated by the degradation of extracellular matrix.[49] In the context of gliomas, this may lead to the generation of a vicious cycle in which TLRs induce and enhance metalloprotease activity that in turn leads to a positive regulation of the TLR signaling, thus boosting glioma pathology.

TLRs form dimers to initiate their signaling, by forming either homodimers with themselves or heterodimers with other TLR subtypes. TLR2 can heterodimerize with TLR1 or TLR6[50] to induce a MyD88-dependent signaling cascade. Indeed, we observed that microglia derived from TLR1- and TLR6-deficient mice showed a reduction in MT1-MMP gene expression upon stimulation with GCM when compared with WT mice, indicating that TLR1 and TLR6 are potential partners required for mediating TLR2 signaling in GAMs. Glioma-released factor(s) influence GAMs via TLR2 signaling to increase MT1-MMP gene and protein expression and thereby contribute to tumor expansion. Results from our current study identified TLRs, especially TLR2 expressed by GAMs, as a promising and potential target for immune-based treatment options for glioma patients. Indeed, hampering glioma-controlled intracellular pathways of microglia activation with a drug such as minocycline[11,40] or propentofylline[51] has the potential to impair experimental glioma growth in mice. We anticipate that these and other studies in the future will initiate clinical trials to target glioma-associated microglia/brain macrophages TLRs for successful treatment of malignant gliomas.

Supplementary Material

Supplementary material is available at *Neuro-Oncology Journal* online (http://neuro-oncology.oxfordjournals.org/).

Acknowledgments

We are thankful to Dr Nico van Rooijen for providing us with liposome-encapsulated clodronate for microglial cell depletion. We sincerely thank Sabrina Lehmann, Karen Rosenberger, and Katja Drekow for their extensive help in providing TLR 2, 7, and 9 KO mice from Charité, Berlin. Many thanks to Irene Haupt, Regina Piske, and Nadine Scharek for excellent technical assistance and Pina Knauff for helping with real-time qPCRs. We thank Dr Zoltan Cseresnyes and Dr Anje Sporbert for their help on the confocal microscope. Words of sincere gratitude to Dr Christina Eichhorn for all her help with some of the statistical analyses in our study.

Conflict of interest statement. None declared.

Funding

This work was supported by a Deutsche Akademischer Austausch Dienst stipend (DAAD, Germany) to Katyayni Vinnakota, a China Scholarship Council stipend (CSC, China) to Feng Hu, and by the Deutsche Forschungsgemeinschaft (SFB TRR43 and Neurocure).

References

1. Ohgaki H, Kleihues P. Epidemiology and etiology of gliomas. *Acta Neuropathol*. 2005;109(1):93–108.
2. Alves TR, Lima FR, Kahn SA, et al. Glioblastoma cells: a heterogeneous and fatal tumor interacting with the parenchyma. *Life Sci*. 2011; 89(15–16):532–539.
3. Charles NA, Holland EC, Gilbertson R, Glass R, Kettenmann H. The brain tumor microenvironment. *Glia*. 2011;59(8):1169–1180.
4. Persano L, Rampazzo E, Della Puppa A, Pistollato F, Basso G. The three-layer concentric model of glioblastoma: cancer stem cells, microenvironmental regulation, and therapeutic implications. *Scientific WorldJournal*. 2011;11:1829–1841.
5. Kettenmann H, Hanisch UK, Noda M, Verkhratsky A. Physiology of microglia. *Physiol Rev*. 2011;91(2):461–553.
6. Hanisch UK, Kettenmann H. Microglia: active sensor and versatile effector cells in the normal and pathologic brain. *Nat Neurosci*. 2007;10(11): 1387–1394.
7. Giometto B, Bozza F, Faresin F, Alessio L, Mingrino S, Tavolato B. Immune infiltrates and cytokines in gliomas. *Acta Neurochir (Wien)*. 1996;138(1):50–56.
8. Watters JJ, Schartner JM, Badie B. Microglia function in brain tumors. *J Neurosci Res*. 2005;81(3):447–455.
9. Kreutzberg GW. Microglia: a sensor for pathological events in the CNS. *Trends Neurosci*. 1996;19(8):312–318.
10. Li W, Graeber MB. The molecular profile of microglia under the influence of glioma. *Neuro Oncol*. 2012;14(8):958–978.
11. Markovic DS, Glass R, Synowitz M, Rooijen N, Kettenmann H. Microglia stimulate the invasiveness of glioma cells by increasing the activity of metalloprotease-2. *J Neuropathol Exp Neurol*. 2005;64(9): 754–762.
12. Markovic DS, Vinnakota K, Chirasani S, et al. Gliomas induce and exploit microglial MT1-MMP expression for tumor expansion. *Proc Natl Acad Sci U S A*. 2009;106(30):12530–12535.
13. Markovic DS, Vinnakota K, van Rooijen N, et al. Minocycline reduces glioma expansion and invasion by attenuating microglial MT1-MMP expression. *Brain Behav Immun*. 2011;25(4):624–628.
14. Moresco EM, LaVine D, Beutler B. Toll-like receptors. *Curr Biol*. 2011;21(13):R488–R493.
15. Takeda K, Kaisho T, Akira S. Toll-like receptors. *Annu Rev Immunol*. 2003;21:335–376.
16. Uematsu S, Akira S. Toll-like receptors and innate immunity. *J Mol Med (Berl)*. 2006;84(9):712–725.
17. Iwasaki A, Medzhitov R. Toll-like receptor control of the adaptive immune responses. *Nat Immunol*. 2004;5(10):987–995.
18. Devaraj S, Dasu MR, Rockwood J, Winter W, Griffen SC, Jialal I. Increased toll-like receptor (TLR) 2 and TLR4 expression in monocytes from patients with type 1 diabetes: further evidence of a proinflammatory state. *J Clin Endocrinol Metab*. 2008;93(2):578–583.
19. Dasu MR, Ramirez S, Isseroff RR. Toll-like receptors and diabetes: a therapeutic perspective. *Clin Sci (Lond)*. 2012;122(5):203–214.
20. Kim S, Karin M. Role of TLR2-dependent inflammation in metastatic progression. *Ann N Y Acad Sci*. 2011;1217:191–206.
21. Szajnik M, Szczepanski MJ, Czystowska M, et al. TLR4 signaling induced by lipopolysaccharide or paclitaxel regulates tumor survival and chemoresistance in ovarian cancer. *Oncogene*. 2009;28(49): 4353–4363.
22. Hansson GK, Lundberg AM. Toll in the vessel wall—for better or worse? *Proc Natl Acad Sci U S A*. 2011;108(7):2637–2638.
23. Vallejo JG. Role of toll-like receptors in cardiovascular diseases. *Clin Sci (Lond)*. 2011;121(1):1–10.
24. Anders HJ, Banas B, Schlondorff D. Signaling danger: toll-like receptors and their potential roles in kidney disease. *J Am Soc Nephrol*. 2004;15(4):854–867.
25. Farrar CA, Keogh B, McCormack W, et al. Inhibition of TLR2 promotes graft function in a murine model of renal transplant ischemia-reperfusion injury. *FASEB J*. 2011;26(2):799–807.
26. Siggers RH, Hackam DJ. The role of innate immune-stimulated epithelial apoptosis during gastrointestinal inflammatory diseases. *Cell Mol Life Sci*. 2011;68(22):3623–3634.
27. Cario E. Innate immune signalling at intestinal mucosal surfaces: a fine line between host protection and destruction. *Curr Opin Gastroenterol*. 2008;24(6):725–732.
28. Fresno M, Alvarez R, Cuesta N. Toll-like receptors, inflammation, metabolism and obesity. *Arch Physiol Biochem*. 2011;117(3):151–164.
29. Butchi NB, Woods T, Du M, Morgan TW, Peterson KE. TLR7 and TLR9 trigger distinct neuroinflammatory responses in the CNS. *Am J Pathol*. 2011;179(2):783–794.
30. Grauer OM, Molling JW, Bennink E, et al. TLR ligands in the local treatment of established intracerebral murine gliomas. *J Immunol*. 2008;181(10):6720–6729.
31. Takeuchi O, Hoshino K, Kawai T, et al. Differential roles of TLR2 and TLR4 in recognition of gram-negative and gram-positive bacterial cell wall components. *Immunity*. 1999;11(4):443–451.

32. Takeuchi O, Kawai T, Muhlradt PF, et al. Discrimination of bacterial lipoproteins by Toll-like receptor 6. *Int Immunol*. 2001;13(7):933–940.
33. Takeuchi O, Sato S, Horiuchi T, et al. Cutting edge: role of Toll-like receptor 1 in mediating immune response to microbial lipoproteins. *J Immunol*. 2002;169(1):10–14.
34. Hemmi H, Kaisho T, Takeuchi O, et al. Small anti-viral compounds activate immune cells via the TLR7 MyD88-dependent signaling pathway. *Nat Immunol*. 2002;3(2):196–200.
35. Hemmi H, Takeuchi O, Kawai T, et al. A Toll-like receptor recognizes bacterial DNA. *Nature*. 2000;408(6813):740–745.
36. Prinz M, Hanisch UK. Murine microglial cells produce and respond to interleukin-18. *J Neurochem*. 1999;72(5):2215–2218.
37. Nolte C, Moller T, Walter T, Kettenmann H. Complement 5a controls motility of murine microglial cells in vitro via activation of an inhibitory G-protein and the rearrangement of the actin cytoskeleton. *Neuroscience*. 1996;73(4):1091–1107.
38. Van Rooijen N, Sanders A. Liposome mediated depletion of macrophages: mechanism of action, preparation of liposomes and applications. *J Immunol Methods*. 1994;174(1–2):83–93.
39. Paxinos G, Franklin K. The Mouse Brain in Stereotaxic Coordinates. 2nd ed. San Diego: Academic Press; 2001.
40. Glass R, Synowitz M, Kronenberg G, et al. Glioblastoma-induced attraction of endogenous neural precursor cells is associated with improved survival. *J Neurosci*. 2005;25(10):2637–2646.
41. Gabrusiewicz K, Ellert-Miklaszewska A, Lipko M, Sielska M, Frankowska M, Kaminska B. Characteristics of the alternative phenotype of microglia/macrophages and its modulation in experimental gliomas. *PloS One*. 2011;6(8):e23902.
42. Beutler B, Hoebe K, Shamel L. Forward genetic dissection of afferent immunity: the role of TIR adapter proteins in innate and adaptive immune responses. *C R Biol*. 2004;327(6):571–580.
43. Olson JK, Miller SD. Microglia initiate central nervous system innate and adaptive immune responses through multiple TLRs. *J Immunol*. 2004;173(6):3916–3924.
44. Lehnardt S. Innate immunity and neuroinflammation in the CNS: the role of microglia in Toll-like receptor-mediated neuronal injury. *Glia*. 2010;58(3):253–263.
45. Bassi R, Giussani P, Anelli V, et al. HMGB1 as an autocrine stimulus in human T98G glioblastoma cells: role in cell growth and migration. *J Neurooncol*. 2008;87(1):23–33.
46. Gately CL, Muul LM, Greenwood MA, et al. In vitro studies on the cell-mediated immune response to human brain tumors. II. Leukocyte-induced coats of glycosaminoglycan increase the resistance of glioma cells to cellular immune attack. *J Immunol*. 1984;133(6):3387–3395.
47. Guzhova I, Kislyakova K, Moskaliova O, et al. In vitro studies show that Hsp70 can be released by glia and that exogenous Hsp70 can enhance neuronal stress tolerance. *Brain Res*. 2001;914(1–2):66–73.
48. Curtin JF, Liu N, Candolfi M, et al. HMGB1 mediates endogenous TLR2 activation and brain tumor regression. *PLoS Med*. 2009;6(1):e10.
49. Johnson GB, Brunn GJ, Platt JL. Cutting edge: an endogenous pathway to systemic inflammatory response syndrome (SIRS)-like reactions through Toll-like receptor 4. *J Immunol*. 2004;172(1):20–24.
50. Farhat K, Riekenberg S, Heine H, et al. Heterodimerization of TLR2 with TLR1 or TLR6 expands the ligand spectrum but does not lead to differential signaling. *J Leukoc Biol*. 2008;83(3):692–701.
51. Jacobs VL, Landry RP, Liu Y, Romero-Sandoval EA, De Leo JA. Propentofylline decreases tumor growth in a rodent model of glioblastoma multiforme by a direct mechanism on microglia. *Neuro Oncol*. 2011;14(2):119–131.